

# Experimental studies on reducing permanent magnet losses through segmentation in a fractional slot PMSM with high power density

Tomasz WOLNIK<sup>1</sup>, Tomasz JAREK<sup>1</sup>, Jan MIKOŚ<sup>1\*</sup>, and Vítězslav STYSKALA<sup>2</sup>

<sup>1</sup> Łukasiewicz Research Network – Upper Silesian Institute of Technology, 44-100 Gliwice, Poland

<sup>2</sup> Department of Electrical Power Engineering, VSB-Technical University of Ostrava, 708 00 Ostrava-Poruba, Czech Republic

**Abstract.** The paper presents the results of numerical calculations and experimental tests on reducing eddy current losses in permanent magnets by means of segmentation in a high-power fractional slot PMSM. This type of motor allows for obtaining a high value of specific power (kW/kg), but at the same time they are characterized by the problem of eddy current losses in rotor elements. Thus designed and manufactured model of motor, which is the subject of this work, has a maximum power of 50 kW (at 4800 rpm) and a mass of 10.5 kg. Reducing eddy current losses by segmentation of permanent magnets is a well-known and widely described method, but there is a lack of papers showing the results of experimental studies, in particular of high-power density motors. This article presents results of the effectiveness of reducing eddy current losses for several variants of axial and circumferential segmentation. The results of experimental studies were verified and compared with the results of numerical calculations performed in the ANSYS Motor-CAD software.

**Keywords:** eddy current losses; segmentation of permanent magnets; high power density motors.

## 1. INTRODUCTION

One of the current significant challenges in the field of electrical drives is the application of electric units in aviation [1–5]. For this type of applications, small dimensions and weight are required, and at the same time high operating parameters of the motor are a must, e.g. specific power, which is the coefficient that determines the ratio of the motor power  $P_{\text{shaft}}$  to its weight, expressed in the unit of W/kg [1]. A high specific power coefficient is achieved, among other things, by increasing the number of magnetic poles of the motor, and thus increasing the frequency of its supply voltage [6, 7]. Fractional slot concentrated winding (FSCW) motors have very good properties due to the possibility of making machines with a large number of magnetic poles and a relatively small number of stator slots. It provides for the possibility of reducing the diameter of the stator core [7, 8]. In addition, FSCW motors are also characterized by lower phase resistance of the windings due to smaller end-connections, thus experiencing lower copper losses and having smaller mass [cite9]. A significant disadvantage of this type of construction, however, is the content of higher harmonics and subharmonics in the distribution of the magnetomotive force (MMF). They are the cause of eddy current losses in the rotor elements, including in permanent magnets (PM), especially intensified in the case of high power density motors, due to the operating conditions with high current loads and high supply frequencies [8, 9]. In certain situations, especially in the case of

incorrect selection of the slot – pole combinations, these losses may cause excessive heating of rotor elements, leading, in extreme cases, to demagnetization of permanent magnets [8]. On the other hand, the selection of slot-pole combinations also significantly affects the motor noise, which should also be taken into account [10]. There are known design methods that allow for limiting the phenomenon of inducing eddy current losses in rotor elements [11]. One of the well-recognized methods is the segmentation of permanent magnets, described, among others, in papers [12–23].

General information and the causes of eddy current losses in permanent magnets were described by the authors in [19]. The influence of axial and circumferential segmentation on losses generated in permanent magnets for PMSMs (permanent magnet synchronous motors) operating at low power supply frequencies has been presented in works [12, 13]. The analysis shows that circumferential segmentation reduces losses generated in permanent magnets  $\Delta P_{\text{PM}}$  to a greater extent than in the case of axial segmentation. The division of magnets in the radial direction into equal and unequal parts was proposed by the authors in [14]. However, for the case of FSCW PMSM, this solution does not bring beneficial results. In works [15, 18], the authors examine the impact of magnet segmentation for PMSMs for various stator winding configurations (multi-phase and multi-layer systems, concentrated windings) and the location of the magnets in the rotor (SPM, IPM, inset). In publications [16, 17], the authors introduce correction coefficient for 2D field analyses, which can be used to obtain distinctly greater convergence of the results of 2D numerical calculations with real measurements. The ANSYS Motor-CAD software uses the formula for the correction coefficient for 2D analyses proposed by the authors in

\*e-mail: [jan.mikos@git.lukasiewicz.gov.pl](mailto:jan.mikos@git.lukasiewicz.gov.pl)

Manuscript submitted 2024-09-30, revised 2024-12-02, initially accepted for publication 2024-12-16, published in July 2025.

publication [17]. The authors in [18] analyze the impact of axial segmentation of magnets for different operating frequencies of the inverter, but their attention was mainly focused on determining the impact of slot harmonics and the carrier wave on the level of loss reduction.

Works [12–18, 20–22], analyzing the impact of segmentation of permanent magnets on the values of eddy current losses, are theoretical works and are based on numerical simulations. These publications do not take into account the specificity and operating/power conditions of the high-power density motor, and the authors do not present experimental verification on the target objects. The literature also lacks a comparative analysis based on the results of experimental tests, determining the impact of permanent magnet segmentation on both, the reduction of magnet losses and the impact on the motor’s operating parameters. In [23], the authors present an experimental verification of the influence of permanent magnet segmentation on the value of eddy current losses, however, it concerns a generator with permanent magnets with completely incomparable operating conditions in relation to a motor with high power density.

The aim of this paper was to experimentally verify and evaluate the effectiveness of the impact of permanent magnet segmentation on the value of eddy current losses in permanent magnets and the impact of individual segmentation variants on the operational parameters and specific power of the FSCW PMSM. The study considered the case of no magnet segmentation (A0C0), 2-stage axial segmentation (A2C0), 4-stage axial segmentation (A4C0) as well as 4-stage axial segmentation with 2-stage circumferential segmentation (A4C2). The results obtained from laboratory tests were compared with the results of numerical calculations both taking into account sinusoidal power supply (theoretical, ideal conditions) and inverter power supply (taking PWM modulation into account).

The object of research is the FSCW PMSM with an external rotor, with a maximum power of 50 kW (@4800 rpm) and a mass of 10.5 kg. The motor has 24 slots in the stator and 20 magnetic poles in the rotor. The rotor core is made of laminated sheets to maximize the reduction of eddy current losses in the rotor core. This way, it can be assumed with some simplification that the eddy current losses induced in the rotor are entirely released in the permanent magnets. Permanent magnets are mounted onto the surface of the rotor yoke (SPM type rotor).

This article is organized as follows. Section 2 presents detailed information about the object under analysis. Section 3 presents the results of numerical calculations for the analyzed variants of permanent magnet segmentation. Section 4 presents the results of laboratory tests carried out on prepared experimental models regarding the impact of permanent magnet segmentation on the reduction of eddy current losses and motor operating parameters. Section 5 compares the results obtained and prepares final conclusions.

## 2. OBJECT OF THE ANALYSIS

The subject of the analysis in this paper is a high pole number FSCW PMSM with an external rotor. The motor weighs approximately 10 kg and reaches a maximum power of 50 kW (@4800 rpm), which generates specific power of 4.7 kW/kg.

Figure 1 shows an illustrative model of the electromagnetic circuit of the motor, used for numerical calculations. The motor is liquid cooled at a flow rate of 8 dm<sup>3</sup>/min and powered by an inverter. The motor has 20 magnetic poles, so for a maximum speed of 4800 rpm, the frequency of the supply voltage is 800 Hz.

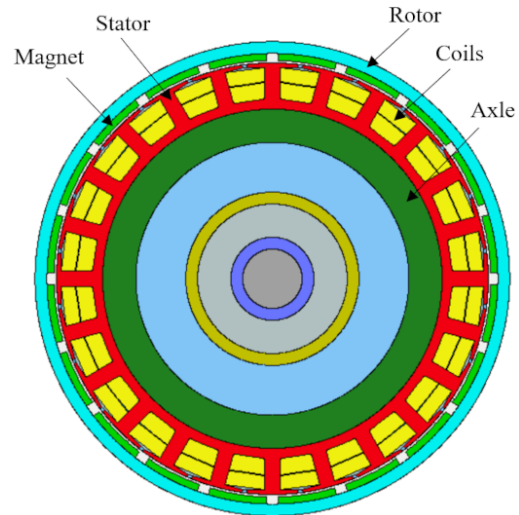


Fig. 1. Illustrative computational model of the motor’s electromagnetic circuit used for numerical calculations

The work analyzed and examined 4 cases of permanent magnet segmentation:

- no magnet segmentation (A0C0),
- 2-stage axial segmentation (A2C0),
- 4-stage axial segmentation (A4C0),
- 4-stage axial segmentation and 2-stage circumferential segmentation (A4C2).

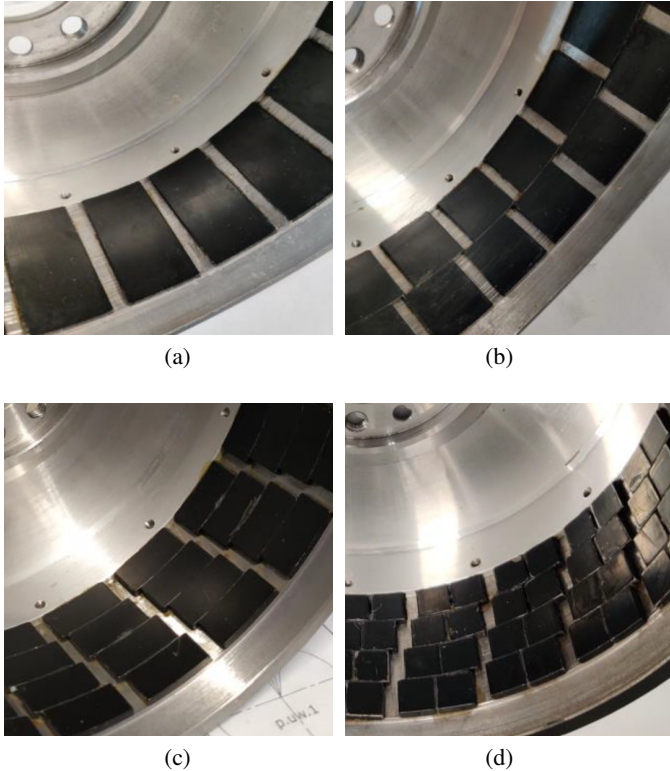
The same stator was used for all cases subject to analysis. Laboratory and simulation tests of all models were carried out

Table 1

Basic data of the analyzed motor

Parameter	Unit	Value
DC supply voltage	V	200
Rotational speed range	rpm	0–4800
Rated current	Arms	240
Outer diameter of rotor core	mm	200
Number of poles	–	20
Number of slots	–	24
Pole arc coefficient	–	0.833
Rotor yoke material type	–	Laminated, M400-50A
Stator core material type	–	N027, 0.27 mm
Type of PM	–	N45SH
Thickness of PM	mm	3
Dimensions of PM (A0C0)	mm	Length – 50, Width – 24.8
Flux weakening	–	none
Winding type	–	Concentrated, double-layer

for identical power supply, cooling and load conditions. Only various rotor solutions were subject to changes, the physical models of which were presented in Fig. 2. Table 1 shows the basic motor data common to all analyzed cases.



**Fig. 2.** Experimental models of rotors analyzed in this work: (a) A0C0, (b) A2C0, (c) A4C0, (d) A4C2

### 3. NUMERICAL SIMULATIONS – SEGMENTATION OF PERMANENT MAGNETS

Obtaining a high specific power of the motor requires taking into account operation with relatively high temperature values, mainly in the winding. High current density (15–30 A/mm<sup>2</sup>) and high frequency of the supply voltage (up to 1000 Hz) are also often the reason for power losses in the rotor elements. Segmentation of permanent magnets is one of the effective ways to reduce power losses in the magnets, but it causes greater technological complexity and workload. For this reason, it is important to properly select the level of segmentation depending on the motor operating conditions and the relevant need to reduce the level of eddy current losses in the magnets to prevent overheating. As part of this article, numerical simulations were performed for the variants of the rotor solution being analyzed, taking into account the thermal model in ANSYS Motor-CAD. This software enables the calculation of losses in permanent magnets for every case of rotor variants and the connection of the electromagnetic module with the thermal module. Knowledge about the temperature distribution in motor components at the stage of designing the electromagnetic circuit leads to obtaining the most advantageous solution possible among the cases considered. In the first stage of the simulations, the impact of permanent magnet

segmentation on the value of losses generated was examined, taking into account that the motor is supplied by an ideal source of sinusoidal alternating current  $I_{RMS} = 240$  A and frequency  $f = 800$  Hz. Simulations were carried out taking into account the thermal model in order to reproduce the temperature distribution. When designing the motor, the loss magnification factor in the rotor and stator iron was assumed to be 1.8, and for permanent magnets it stood at 2. Such loss magnification values are commonly used when designing motors with permanent magnets. Table 2 presents the simulation results obtained for the cases analyzed, where  $\vartheta_{PM}$  is the average temperature of PM,  $\Delta P_{PM}$  stands for losses in PM,  $P_{shaft}$  is shaft power,  $\Delta P_{TotalLosses}$  are total power losses in the motor, and  $\eta$  is motor efficiency.

**Table 2**

Results of numerical simulations when the motor is powered by sinusoidal current,  $I_{RMS} = 240$  A,  $f = 800$  Hz

Segmentation	$\vartheta_{PM}$ [°C]	$\Delta P_{PM}$ [W]	$P_{shaft}$ [kW]	$\Delta P_{TotalLosses}$ [W]	$\eta$ [%]
A0C0	109.7	772	30.7	2400	92.8
A2C0	100.9	672	30.7	2300	93.0
A4C0	67.7	288	31.2	1900	94.0
A4C2	81.2	446	30.9	2100	93.7

The results presented in Table 2 show that the most advantageous variant is A4C0 segmentation. Compared to the A0C0 variant, losses in the magnets have been reduced by 63%. For the A4C2 rotor, the level of calculated power losses in the magnets increased by as much as 55% compared to the A4C0 model, which was considered to require further explanation and appeared inconsistent with the current state of the art. The reason for the discrepancy may be formula (1) for the correction coefficient  $F$  of losses in magnets in 2D analyses, used by the ANSYS Motor-CAD software [17]. The denominator of the formula being presented is the width of the magnet  $w$ , which, if reduced, results in the increase of the correction coefficient. It is assumed that for the analyzed project this is the reason for the results obtained, which are not theoretically confirmed in the literature.

$$F = \frac{3}{4} \cdot \frac{L^2}{w^2 + L^2}, \quad (1)$$

where  $F$  is the correction coefficient,  $w$  is magnet transversal width, and  $L$  is axial length of 1 magnet block.

Under real operating conditions, the motor is powered by an inverter, which generates a number of higher harmonics in the supply current, resulting in increased losses, among others, in permanent magnets. For this reason, numerical simulations were also performed taking into account PWM modulation and the distorted supply current waveform. The course of this current is shown in Fig. 3. The current waveform is given in relative units relating to the value of the effective rated current of 240 A. The calculation results for the analyzed magnet segmentation variants are presented in Table 3.

The application of higher harmonics in the supply current resulted in an increase in the loss in the permanent magnets by

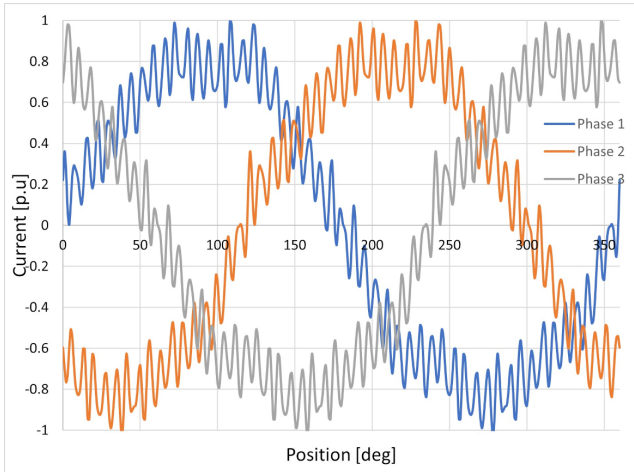


**Fig. 3.** Current waveform when powered by an inverter as a function of the rotor position

**Table 3**

Results of numerical simulations when supplying the motor with current, taking account of PWM modulation,  $I_{RMS} = 240$  A,  $f = 800$  Hz

Segmentation	$\vartheta_{PM}$ [°C]	$\Delta P_{PM}$ [W]	$P_{shaft}$ [kW]	$\Delta P_{TotalLosses}$ [W]	$\eta$ [%]
A0C0	143.2	1107	29.2	2880	91.0
A2C0	113.1	771	29.5	2540	92.0
A4C0	76.2	350	30.2	2120	93.4
A4C2	88.7	504	30.0	2270	92.9

43% for A0C0, by 15% for A2C0, by 21% for A4C0 and by 13% for A4C2. Such a significant increase in losses in the magnets in the A0C0 variant resulted in the calculated temperature value in the permanent magnets  $\vartheta_{PM}$  being 143°C, which is almost the limit temperature. At such high temperatures, the magnet is exposed to demagnetization. Performing axial segmentation (A4C0) reduced the magnet temperature by as much as 67 K. Similarly to the case of sinusoidal current supply, the calculated values of losses in magnets for the A4C2 case are higher than A4C0, which is not consistent with the theoretical assumptions. The calculated temperature distribution for individual magnet segmentations is presented in Fig. 4.

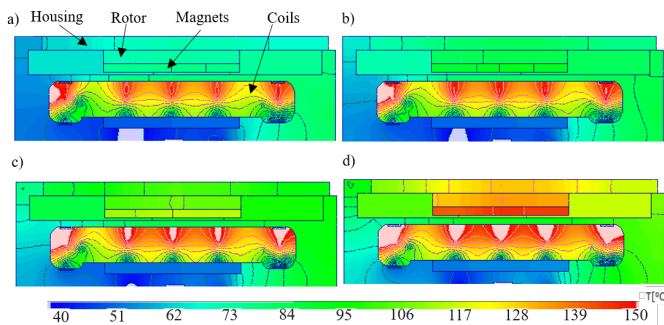


**Fig. 4.** Temperature distribution in the elements of the electromagnetic circuit for the analyzed variants of the rotor: (a) A4C0, (b) A4C2, (c) A2C0, (d) A0C0

The numerical simulations also included an analysis of the influence of changes in the motor current at a constant rotor speed  $n = 4800$  rpm (800 Hz) on the temperature generated in the permanent magnets (Fig. 5).

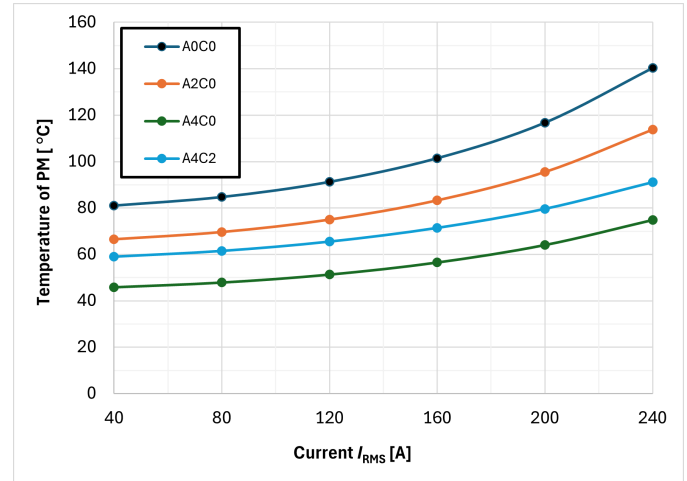


**Fig. 5.** Calculated dependence of the temperature of permanent magnets as a function of motor current changes for the analyzed segmentation variants

#### 4. LABORATORY TEST RESULTS

Laboratory tests were performed to examine the impact of segmentation of permanent magnets on eddy current losses. This section presents the test results for all analyzed rotor models. Direct measurement of losses in permanent magnets on a test stand is not possible for a motor with rotating parts. Indirect methods involving the division of individual losses in the tests carried out could be subject to quite large errors, introducing uncertainty into the results obtained. It was therefore decided that the best way to reflect the level of losses emitted in permanent magnets (it is assumed that due to the packaged rotor, losses in the core are negligible) is to directly measure the temperature of the permanent magnets. Assuming the same load, power supply and cooling conditions for all analyzed models, it can also be assumed that the temperature increase in permanent magnets resulting from heat transfer from the stator part to the rotor is the same for all cases. In order to measure the temperature in the permanent magnets, Pt100 temperature sensors with wires led outside the rotor were installed in each of the rotor models (Fig. 6). After each completed heating test (after stabilization of temperature values at all measurement points), carried out for specific power and load conditions, the temperature of the permanent magnets was directly measured. During each heating test, the temperature of the stator windings was also continuously recorded (at five measurement points: D end winding, ND end winding, U phase slot, V phase slot, W phase slot), and continuous recording of rotor surface temperature was performed. For this purpose, a specially developed solution of a wireless temperature recorder with an installed infrared sensor was used, directed at the external surface of the rotor during motor operation. The recorder is battery-powered with contin-

uous monitoring of the charge level. It also has the ability to continuously record temperature values to non-volatile memory with the ability to easily download the results.



Fig. 6. Temperature sensors mounted on permanent magnets and placed outside the rotor

Laboratory tests were carried out with the motor supply by rated current  $I_{RMS} = 240$  A and variable rotation speed in the range of 600–4800 rpm. The diagram of the measurement system of the tested motor is shown in Fig. 7. The tested motor was coupled with the auxiliary machine and torque meter, and connected to the motor controller. In addition to the above-described stator and rotor temperature measurements, motor currents and voltages as well as shaft speed and torque were measured by a precision power analyzer. Based on these, the active power, shaft power and motor efficiency were determined.

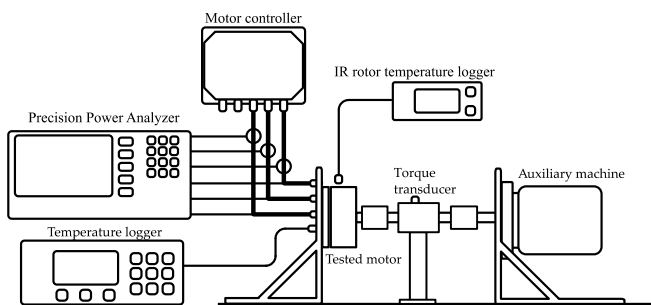


Fig. 7. Measurement system of the analyzed motor

Figures 8–10 present the measured characteristics of permanent magnet temperature  $\vartheta_{PM}$ , total losses  $\Delta P_{TotalLosses}$  and motor efficiency  $\eta$  for individual rotor variants: A0C0, A2C0, A4C0 and A4C2. Table 4 presents the measured power values on the motor shaft for the rated load for the subsequent magnet segmentation solutions analyzed in this work. It should be noted that for the A0C0 case, there is no skew in the rotor due to only one magnet used. The stator for all tested variants was the same, so it also does not take into account the skew of the slots. Due to the above, the measured torque on the motor shaft was multiplied by the calculated skew factor, which was 0.955 for

the analyzed motor, so as to ensure comparability of the results for all the cases analyzed.

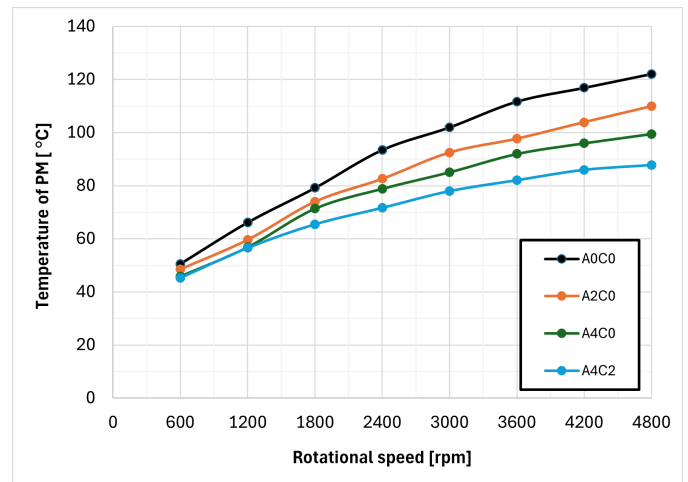


Fig. 8. Measured temperature of permanent magnets for rated current  $I_{RMS} = 240$  A

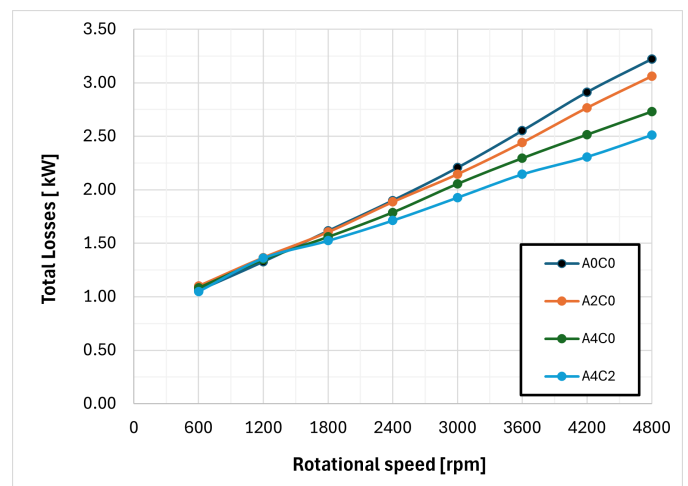


Fig. 9. Total power loss for rated current  $I_{RMS} = 240$  A

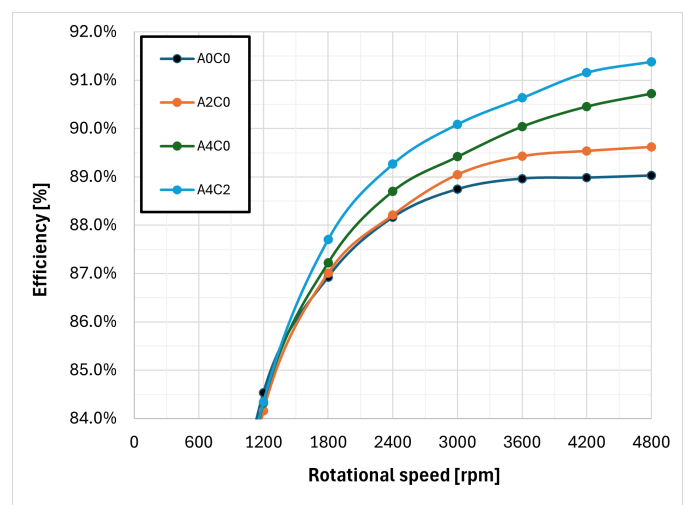


Fig. 10. Motor efficiency for rated current  $I_{RMS} = 240$  A

**Table 4**Shaft power for rated current  $I_{RMS} = 240$  A

$n$ [rpm]	A0C0 $P_{shaft}$ [kW]*	A2C0 $P_{shaft}$ [kW]	A4C0 $P_{shaft}$ [kW]	A4C2 $P_{shaft}$ [kW]
600	3.67	3.67	3.67	3.72
1200	7.26	7.26	7.25	7.34
1800	10.74	10.75	10.65	10.88
2400	14.15	14.11	14.05	14.25
3000	17.40	17.45	17.37	17.52
3600	20.58	20.66	20.75	20.76
4200	23.53	23.68	23.84	23.79
4800	26.15	26.44	26.71	26.64

\* measured shaft torque multiplied by the skew factor

When analyzing the results presented in Table 4, we notice that in the speed range of 600–2400 rpm, the segmentation of permanent magnets does not significantly affect the value of the motor output power. This is the result of relatively small differences in the temperature of the permanent magnets, which ranges is from 71.7°C to 93.5°C. The tendency of increasing the output power with increasing the degree of segmentation is observed in the motor operating range of 3000–4800 rpm, i.e. when the rotor temperature differences between the individual variants increase significantly and are in the range of 87.8–122.1°C. The measured increase in output power on the motor shaft is approximately 550 W for extreme cases, which is an increase of approximately 2%.

In turn, analyzing the characteristics presented in Figs. 8–10 we can notice that the segmentation of permanent magnets significantly reduced the temperature of the magnets, especially for the maximum rotational speed of 4800 rpm (800 Hz). The lowest temperature was obtained for the A4C2 case, i.e. 87.8°C, while the highest value was obtained for the A0C0 variant, i.e. 122.1°C. The difference is therefore as much as 34.3 K. Such a large temperature reduction is the result of a significant reduction in power losses in permanent magnets. Tests of all variants were carried out for an identical armature, with the same power supply parameters and load conditions. It can therefore be assumed that the measured value of the difference in total losses (Fig. 9) relates entirely to the losses released in the permanent magnets. For the current  $I_{RMS} = 240$  A and  $n = 4800$  rpm, the difference between the two extreme cases A0C0 and A4C2 is as much as 710 W. This, of course, results in a significant difference in the efficiency of the motor: 89.0% for A0C0 and 91.4 % for A4C2.

## 5. CONCLUSIONS

The issue analyzed in this work is experimental research on the impact of permanent magnet segmentation on the losses and temperature of the magnets and operational parameters of the high power density PMSM. Magnet segmentation is a well-known method, widely described in the literature, but there is no work based on the results of experimental research. Most of the

work is based on simulation models, which, moreover, have not yet included a detailed analysis in the context of high-power density motors. As part of this work, laboratory tests were carried out for PMSM with a maximum power of 50 kW (@4800 rpm) and a mass of 10.5 kg for four rotor models with different stage of permanent magnet segmentation: A0C0, A2C0, A4C0 and A4C2. Additionally, numerical simulations were performed for comparison purposes. Table 5 compares the simulation results and laboratory test results in terms of permanent magnet temperature, output power and motor efficiency.

**Table 5**Comparison of the results of numerical simulations with the results of laboratory tests for  $I_{RMS} = 240$  A,  $n = 4800$  rpm

		A0C0*	A2C0	A4C0	A4C2
$\vartheta_{PM}$ [°C]	Calc.	143.2	113.1	76.2	88.7
	Test	122.1	109.9	99.5	87.8
$P_{shaft}$ [kW]	Calc.	29.2	29.5	30.2	30.0
	Test	26.2	26.4	26.7	26.6
$\eta$ [%]	Calc.	91.0	92.0	93.4	92.9
	Test	89.0	89.6	90.7	91.4

\* measured shaft torque multiplied by the skew factor

Referring to the results presented in Table 5, the following issues should be noted:

- Quite significant differences between the calculated and measured temperatures of permanent magnets are noticeable. Discrepancies in the results obtained may be caused by differences between the complex computational thermal model and the actual motor model. The thermal model of the motor in ANSYS Motor-CAD requires consideration of thermal conductivity of the materials and the resistance of the contacts between the components, which may differ in the actual model. Despite the consistent tendency of decreasing magnet temperature with increasing segmentation stage, similar results were obtained only for the A4C2 case.
- There are noticeable differences between the calculated and measured motor efficiency. For each of the analyzed variants, the difference between calculations and measurements is 1.5–3% efficiency. In this case, however, there is a high convergence of the tendency to increase efficiency with the increase in the degree of segmentation of permanent magnets.
- The results of numerical calculations showed that the application of circumferential segmentation (A4C2) resulted in an increase in losses and temperature in the magnets as compared with the variant without circumferential segmentation (A4C0). The result was considered a significant calculation error of the ANSYS Motor-CAD software, which was confirmed during laboratory tests. The introduction of peripheral segmentation actually resulted in a reduction in the temperature of the magnets by 11.7 K and a reduction in losses by approximately 220 W (Fig. 9).

Summarizing the entire issue in this paper, the following conclusions can be drawn:

- Segmentation of permanent magnets allows for a significant reduction in power losses and thus the temperature of permanent magnets in a high-power density motor. For the variants analyzed, the temperature reduction between the most extreme cases was 34.3 K.
- Due to the multi-pole nature of the motor and therefore the small dimensions of the magnets, the technological complexity in the case of introducing circumferential segmentation (A4C2) is disproportionate to the benefits obtained. The temperature difference of the magnets between the A4C0 and A4C2 variants was 11.7 K. Technological difficulties are mainly related to the laborious bonding of relatively small permanent magnets and at the same time maintaining properly assumed dimensional tolerances.
- The results of numerical calculations do not converge satisfactorily with the results of laboratory tests. The only consistency was observed in terms of the trends in the results obtained, but not in terms of numerical values.
- The increased temperature of permanent magnets in the absence of segmentation leads to extenuation of the operating parameters of a high-power density motor, especially in terms of motor efficiency. The difference between the most extreme variants was 2.4% efficiency.

## ACKNOWLEDGEMENTS

This paper was supported and financed by the National Centre for Research and Development (NCBR – Poland), under project LIDER/31/0169/L-12/20/NCBR/2021.

## REFERENCES

- [1] R.C. Bolam, Y. Vagapov, and A. Anuchin, “A Review of Electrical Motor Topologies for Aircraft Propulsion,” in *2020 55th International Universities Power Engineering Conference (UPEC)*, Torino, Italy, Sep. 2020, pp. 1–6. doi: [10.1109/UPEC49904.2020.9209783](https://doi.org/10.1109/UPEC49904.2020.9209783).
- [2] T. Wolnik, T. Jarek, J. Golec, R. Topolewski, and D. Jastrzębski, “High Power Density Motor for Light Electric Aircraft – Design Study and Lab Tests,” *2023 IEEE Workshop on Electrical Machines Design Control and Diagnosis (WEMDCD)*, pp. 1–6, 2023.
- [3] P. Alvarez, M. Satrustegui, I. Elosegui, and M. Martinez-Iturralde, “Review of High Power and High Voltage Electric Motors for Single-Aisle Regional Aircraft,” *IEEE Access*, vol. 10, pp. 112989–113004, 2022, doi: [10.1109/ACCESS.2022.3215692](https://doi.org/10.1109/ACCESS.2022.3215692).
- [4] X. Zhang and K.S. Haran, “High-specific-power electric machines for electrified transportation applications-technology options,” in *2016 IEEE Energy Conversion Congress and Exposition (ECCE)*, Milwaukee, USA, Sep. 2016, pp. 1–8. doi: [10.1109/ECCE.2016.7855164](https://doi.org/10.1109/ECCE.2016.7855164).
- [5] T. Wolnik, T. Jarek, and L. Cyganik, “Improvement Studies of High Power Density Motor for Aviation and Marine Application,” *2023 23rd International Scientific Conference on Electric Power Engineering (EPE)*, pp. 1–6, 2023.
- [6] P. Dukalski and R. Krok, “Selected aspects of decreasing weight of motor dedicated to wheel hub assembly by increasing number of magnetic poles,” *Energies*, vol. 14, p. 917, 2021.
- [7] T. Wolnik, P. Dukalski, B. Bedkowski, and T. Jarek, “Selected aspects of designing motor for direct vehicle wheel drive,” *Prz. Elektrotechniczny*, vol. 1, no. 4, pp. 152–155, Apr. 2020, doi: [10.15199/48.2020.04.31](https://doi.org/10.15199/48.2020.04.31).
- [8] T. Wolnik, V. Styskala, and T. Mlczak, “Study on the selection of the number of magnetic poles and the slot-pole combinations in fractional slot PMSM motor with a high power density,” *Energies*, vol. 15, no. 1, p. 215, Dec. 2021, doi: [10.3390/en15010215](https://doi.org/10.3390/en15010215).
- [9] A.M. EL-Refaie, “Fractional-slot concentrated-windings synchronous permanent magnet machines: opportunities and challenges,” *IEEE Trans. Ind. Electron.*, 57, 2010, pp. 107–121.
- [10] E. Król and M. Maciążek, “Vibroacoustic analysis methods of permanent magnets synchronous motors,” *Prz. Elektrotechniczny*, vol. 1, no. 11, pp. 220–225, 2022, doi: [10.15199/48.2022.11.45](https://doi.org/10.15199/48.2022.11.45).
- [11] T. Wolnik, S. Opach, Ł. Cyganik, T. Jarek, and V. Szekeres, “Design methods for limiting rotor losses in a fractional slot PMSM motor with high power density,” *Arch. Electr. Eng.*, vol. 71, pp. 963–979, 2022.
- [12] P. Sergeant and A. Van Den Bossche, “Segmentation of magnets to reduce losses in permanent-magnet synchronous machines,” *IEEE Trans. Magn.*, vol. 44, no. 11 (part 2), pp. 4409–4412, 2008, doi: [10.1109/TMAG.2008.2001347](https://doi.org/10.1109/TMAG.2008.2001347).
- [13] M. Mirzaei, A. Binder, and C. Deak, “3D analysis of circumferential and axial segmentation effect on magnet eddy current losses in permanent magnet synchronous machines with concentrated windings,” *19th International Conference on Electrical Machines, ICEM 2010*, Italy, 2010, pp. 1–6, doi: [10.1109/ICEL-MACH.2010.5608182](https://doi.org/10.1109/ICEL-MACH.2010.5608182).
- [14] P. Madina, J. Poza, G. Ugalde, and G. Almandoz, “Analysis of non-uniform circumferential segmentation of magnets to reduce eddy-current losses in SPMSM machines,” in *Proc. 20th International Conference on Electrical Machines, ICEM 2012*, 2012, pp. 79–84, doi: [10.1109/ICEIMach.2012.6349843](https://doi.org/10.1109/ICEIMach.2012.6349843).
- [15] Q. Chen, D. Liang, S. Jia, and X. Wan, “Analysis of multi-phase and multi-layer fractional-slot concentrated-winding on PM eddy current loss considering axial segmentation and load operation,” *IEEE Trans. Magn.*, vol. 54, no. 11, pp. 1–6, 2018, doi: [10.1109/TMAG.2018.2841874](https://doi.org/10.1109/TMAG.2018.2841874).
- [16] T. Fadriansyah, T.D. Strous, and H. Polinder, “Axial segmentation and magnets losses of SMPM machines using 2D FE method,” in *Proc. 20th International Conference on Electrical Machines, ICEM 2012*, 2012, pp. 577–581, doi: [10.1109/ICEL-Mach.2012.6349927](https://doi.org/10.1109/ICEL-Mach.2012.6349927).
- [17] S. Ruoho, T. Santa-Nokki, J. Kolehmainen, and A. Arkkio, “Modeling magnet length in 2-D finite-element analysis of electric machines,” *IEEE Trans. Magn.*, vol. 45, no. 8, pp. 3114–3120, 2009, doi: [10.1109/TMAG.2009.2018621](https://doi.org/10.1109/TMAG.2009.2018621).
- [18] K. Yamazaki and Y. Fukushima, “Effect of eddy-current loss reduction by magnet segmentation in synchronous motors with concentrated windings,” *IEEE Trans. Ind. Appl.*, vol. 47, no. 2, pp. 779–788, 2011, doi: [10.1109/TIA.2010.2103915](https://doi.org/10.1109/TIA.2010.2103915).
- [19] D. Ouamara, and F. Dubas, “Permanent-Magnet Eddy-Current Losses: A Global Revision of Calculation and Analysis,” *Math. Computat. Appl.*, vol. 24, no. 3, p. 67, 2019, doi: [10.3390/mca24030067](https://doi.org/10.3390/mca24030067).

T. Wolnik, T. Jarek, J. Mikoś, and V. Styskala

- [20] J.D. Ede, K. Atallah, G.W. Jewell, J.B. Wang, and D. Howe, "Effect of Axial Segmentation of Permanent Magnets on Rotor Loss in Modular Permanent-Magnet Brushless Machines," *IEEE Trans. Ind. Appl.*, vol. 43, no. 5, pp. 1207–1213, 2007, doi: [10.1109/TIA.2007.904397](https://doi.org/10.1109/TIA.2007.904397).
- [21] A. Wan-Ying Huang, R. Bettayeb, R. Kaczmarek, and J.-C. Vannier, "Optimization of Magnet Segmentation for Reduction of Eddy-Current Losses in Permanent Magnet Synchronous Machine," *IEEE Trans. Energy Convers.*, vol. 25, no. 2, pp. 381–387, Jun. 2010, doi: [10.1109/TEC.2009.2036250](https://doi.org/10.1109/TEC.2009.2036250).
- [22] D.A. Wills and M.J. Kamper, "Reducing PM eddy current rotor losses by partial magnet and rotor yoke segmentation," in *XIX International Conference on Electrical Machines - ICEM 2010*, Italy, Sep. 2010, pp. 1–6, doi: [10.1109/ICELMACH.2010.5607993](https://doi.org/10.1109/ICELMACH.2010.5607993).
- [23] P. Upadhayay and V. Patwardhan, "Magnet eddy-current losses in external rotor permanent magnet generator," in *2013 International Conference on Renewable Energy Research and Applications (ICRERA)*, Spain, Oct. 2013, pp. 1068–1071, doi: [10.1109/ICRERA.2013.6749911](https://doi.org/10.1109/ICRERA.2013.6749911).